Fuel 356 (2024) 129561

Contents lists available at ScienceDirect

Fuel

journal homepage: www.elsevier.com/locate/fuel

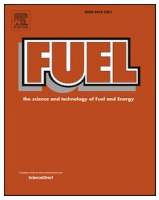

Full Length Article

Experimental measurements of laminar burning velocity of premixed propane-air flames at higher pressure and temperature conditions

Vijay Shinde *, Amardeep Fulzele, Sudarshan Kumar

Department of Aerospace Engineering, Indian Institute of Technology Bombay, Powai, Mumbai 400076, India

ARTICLE INFO

Keywords:
Laminar burning velocity
Propane-air
Diverging channel
Elevated temperature
High pressure

ABSTRACT

This paper presents laminar burning velocity (LBV) measurements of premixed propane-air flames simultaneously at higher mixture pressure (1-5 atm) and temperature (350-630 K) conditions over mixture conditions ($\phi = 0.7$-1.3) utilizing the externally heated diverging channel (EHDC) method. The maximum LBV was observed at $\phi = 1.1$ for all pressure and temperature conditions. The non-monotonic behavior of the temperature exponents was noted with the minima at $\phi = 1.1$. The pressure exponent (β) variation was observed to be parabolic with the maxima at $\phi = 1.0$. The current measurements are then compared with the literature results, and the detailed kinetic model predictions of Qin mech, San Diego mech, and USC mech II. The present LBV measurements are in a better match with the mechanism predictions of San Diego mech at the majority of mixture and pressure conditions. The current measurement suggests the variation of temperature exponent (α) as a function of pressure ratio, and pressure exponent (β) as a function of temperature ratio for different mixture conditions (ϕ). A revised power-law correlation for α and β variations is also suggested as, $S_u = S_{u0}\left(\frac{T_u}{T_{u0}}\right)^{\propto_0+\propto_1\left(1-\frac{P_u}{P_{u0}}\right)}\left(\frac{P_u}{P_{u0}}\right)^{\beta_0+\beta_1\left(1-\frac{T_u}{T_{u0}}\right)}$. The sensitivity analysis reveals a significant increase ($\approx$ 45%) in negative sensitivity for the chain termination reaction H + CH_3 (+M) $\leftrightarrow$ CH_4 (+M) (R56), with a rise in pressure and temperature at all mixture conditions. The reaction pathway analysis indicates a maximum increment in elemental flux ($\approx$ 305 %) in the formation of ethane (C_2H_6) from its predecessor methyl radical (CH_3), due to enhanced pressure and temperature conditions.

1. Introduction

The burning of conventional fossil fuels is a remarkable source of greenhouse gas emissions and air pollution, primarily carbon dioxide (CO_2), which contributes to worldwide weather change. Burning fossil fuels emits huge amounts of CO_2 into the atmosphere, trapping heat and leading to global warming. The burning of fossil fuels also enables the release of other detrimental pollutants, such as sulphur dioxide (SO_2), nitrogen oxides (NO_x), and particulate matter (PM), which can have an unfavourable influence on human health and the environment. To reduce the combustion emissions from fossil fuels, we have to incorporate low hydrocarbon alkane fuels, such as methane, ethane, natural gas, and propane in the existing combustors without compromising the engine efficiency and performance. Propane is a cleaner-burning fuel compared to many conventional fuels, such as coal and oil etc. When combusted, propane generates significantly lower levels of harmful emissions, such as nitrogen oxides, particulate matter, and greenhouse gases [1]. This makes propane a more environmentally friendly fuel option. Propane can be utilized in a broad variety of combustion applications, including heating and power generation in homes, businesses, and industrial settings. It can also be used as a fuel for vehicles and transportation. Propane has a high heating value (46.4 MJ/kg) as compared to gasoline (44 MJ/kg) [2] and can be easily and efficiently burned in combustion systems, producing high temperatures and achieving higher combustion efficiencies. Overall, the advantages of using propane over fossil fuels in combustors include cleaner burning, higher efficiency, versatility, availability and storage, and cost-effectiveness.

Before incorporating propane as an alternative to fossil fuel in the existing combustor, a fundamental combustion study should be carried out, such as laminar burning velocity (LBV), extinction limits, ignition time. The LBV is a vital parameter that characterizes the rate at which a flame front propagates through a combustible mixture. The combustion characteristics of propane, such as LBV, are influenced by various

* Corresponding author.
E-mail address: vijay150976@gmail.com (V. Shinde).

https://doi.org/10.1016/j.fuel.2023.129561
Received 13 May 2023; Received in revised form 20 July 2023; Accepted 18 August 2023

factors, i.e. fuel-air ratio, mixture pressure, and mixture temperature. In some industrial applications, such as gas pipelines and storage tanks, high-pressure, and high-temperature conditions can occur resulting in accidental situations. Understanding the variation of LBV of the propane-air mixture under these conditions is necessary for assessing the risk of fires, flame propagation, or explosions and designing appropriate safety measures. At higher pressure and temperature conditions, such as those encountered in gas turbines, internal combustion engines, and industrial burners, the LBV of a fuel-air mixture can have substantial effects on the combustion efficiency, emissions, and performance of the combustion process. Therefore, a comprehensive understanding of the LBV of the propane-air mixture at higher temperature and pressure conditions is essential for optimizing the design of combustion systems, improving efficiency, reducing emissions, and ensuring safe operation.

Over the decades, different experimental and computational investigations have been conducted to estimate the LBV of the propane-air mixture at elevated temperature and pressure conditions. Experiments have been conducted using various measurement techniques, such as stagnation flame [3], Bunsen flame [4], spherical bomb [5], and heat-flux method [6]. Among these techniques, only the heat flux method is a direct method, which measures the stretch-free LBV at adiabatic conditions. Computational studies [7,8] have also been carried out using various combustion models and numerical techniques to predict the LBV variation of the propane-air mixtures under various conditions.

Metghalchi et al. [9] proposed a power law correlation indicating the influence of pressure and temperature on the LBV measurement of propane-air mixtures utilizing the spherically expanding flame (SEF) method. Hassan et al. [10] carried out the experiments using the SEF method at high pressure and standard condition. They have reported flame instability with pressure due to preferential diffusion. Takizawa and co-workers [11] employed the SEF method to evaluate the LBV of propane-air mixtures. Huzayyin et al. [12] estimated the LBV of propane-air and liquefied petroleum gas (LPG)-air mixtures utilizing the SEF method. They highlighted that propane is more pressure dependent than LPG. Tang et al. [13] obtained the linear variation of the burning velocity and Markstein lengths for C_3H_8-air mixtures with N_2 dilution utilizing the SEF method. Brinzea and co-workers [14–17] evaluated the overall activation energy, reaction orders, and burning velocity of propane-air mixtures using the SEF method. Razus et al. [18] estimated the LBV of C_3H_8-air mixtures using pressure variation in the spherical chamber. The influence of CO_2 dilution on the LBV using the SEF method [19,20] was explored and quantified at various mixture ranges, elevated pressures, and temperature conditions.

Jomaas et al. [21] measured the counterflow ignition temperatures and the LBV of C_2-C_3 hydrocarbon-air mixtures using the counterflow flame method. Akram et al. [22] investigated the effect of CO_2 and N_2 on the premixed propane-air mixture using the externally heated diverging channel (EHDC) method at standard pressure, and higher mixture temperatures. A linear decrease in the LBV was observed for the diluted propane-air mixtures and the influence of carbon dioxide dilution was dominant over the nitrogen case. Goswami et al. [23] measured the LBV of C_2-C_3 alkanes-air flames utilizing the heat-flux method. They observed a significant deviation in pressure exponent (β) with the literature data and kinetic model predictions.

The LBV of a fuel-air mixture at higher pressure and temperature conditions has significant importance in engine design and for the improvement and validation of kinetic models. The LBV depends on the mixture condition (ϕ), unburnt mixture pressure (P_u), and temperature (T_u). The simultaneous effect of pressure and temperature with pressure and temperature exponents on the LBV is shown in Eqn. (1) [24].

$$S_u = S_{u0}\left(\frac{T_u}{T_{u0}}\right)^{\alpha}\left(\frac{P_u}{P_{u0}}\right)^{\beta} \quad (1)$$

where P_{u0} and T_{u0} are standard pressure (1 atm) and temperature (300 K). S_{u0} is the LBV at (P_{u0}, T_{u0}), and S_u is the LBV at pressure P_u and temperature T_u. The β and α are pressure and temperature exponents respectively.

The LBV of the propane-air mixture using different experimental techniques over the last four decades is presented in Table 1. The SEF method is widely used to analyze the effect of pressure on the LBV measurement.

Even though the basic combustion variables of propane-air flames have been considerably examined in previous studies for a broader scale of conditions, there has been little investigation on understanding the simultaneous influence of higher temperature and pressure conditions on the variation of LBV. The pressure exponents (β) are observed for an initial temperature of 300 ± 3 K, and temperature exponents (α) are reported by all researchers for 1 atm pressure at different mixture conditions. Individually, pressure exponents are presumed to be constant at high temperatures, and temperature exponents are assumed to be constant at higher mixture pressures. The detailed LBV measurements performed simultaneously at elevated temperatures and high-pressure conditions would help to understand the effect of mixture temperature on β and mixture pressure on α.

Wang and co-workers [25] carried out the LBV study of methane-air mixtures at engine relevant conditions for methane-air mixtures. Fig. 1 shows a summary of the present LBV studies with the existing literature data along with the thermodynamic conditions encountered in a typical engine during the mixture compression process. In Fig. 1, lines I and II were drawn to imitate the isentropic compression process using the thermodynamic relationship, $T_u/T_{u0} = (P_u/P_{u0})^{(\gamma-1)/\gamma}$, where T_{u0} and P_{u0} are initial temperature and pressure respectively, and γ is the specific heat capacity ratio of the unburned gas. Region 1 between line I and II represents the typical T_u and P_u range during the compression and combustion processes in S.I. engines, and these conditions are considered as engine relevant conditions. Most of the previous studies are carried out in the regions close to lines III and IV. These conditions are referred as unrealistic engine conditions, because they are far away from region 1. However, the present study reports the values of the mixture burning velocity near the engine relevant conditions, (highlighted by yellow colour in Fig. 1). Similar studies at engine relevant conditions using methane-air mixtures were reported by Varghese et al. [26] using EHDC method.

Previous studies for various propane-air mixtures at elevated temperature and atmospheric pressure were conducted by Akram et al. [22]. The present measurements are carried out to analyse the simultaneous effect of the elevated pressure and temperature conditions on the laminar burning velocity of premixed propane-air mixtures using the EHDC method.

Unlike other methods (spherical flame, counterflow, Bunsen flame), which requires flame-stretch extrapolation techniques to extract the unstretched LBV at reference conditions, the EHDC method is a direct

Table 1
A summary of previous literature data in sequential order (1980 onwards) with LBV (S_{u0}), pressure exponent (β), temperature exponent (α), and the operating conditions. SEF - Spherically expanding flame; HF - Heat flux; EHDC - Externally heated diverging channel, NA - not applicable.

Author	Method	T_u (K)	P_u (atm)	ϕ range	S_{u0} (ϕ = 1) (cm/s)	α (ϕ = 1)	β (ϕ = 1)
Metghalchi [9]	SEF	298-750	0.4-40	0.8-1.5	38.31	2.13	-0.17
Takizawa [11]	SEF	280-330	0.8-1.07	0.7-1.4	38.23	1.89	-0.27
Razus [18]	SEF	298-433	0.3-1.97	0.7-1.6	38.95	1.276	-0.163
Akram [22]	EHDC	370-650	1	0.7-1.3	41.87	1.625	NA
Goswami [23]	HF	298	1-4	0.8-1.3	39.6	NA	-0.278

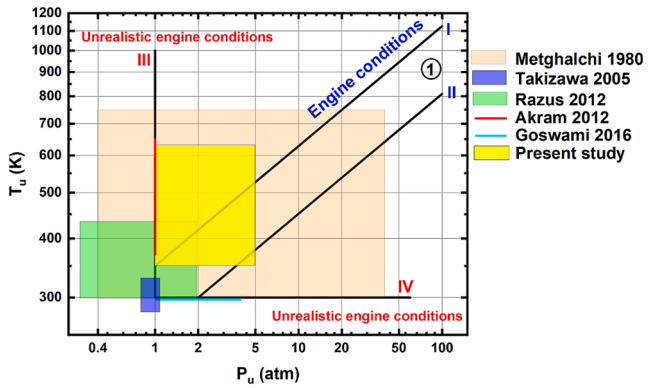

Fig. 1. Summary of experimental conditions for the LBV measurement in the present work and its comparison with literature data.

measurement method (like heat-flux method) to estimate the nearly adiabatic and stretch-free LBV. Hence, the present method helps minimizes the error in LBV measurements at high pressure and high temperature conditions.

The LBV data of the propane-air mixtures at elevated temperature and atmospheric pressure as well as standard temperature and elevated pressure conditions are available in the literature. However, very few studies (Metghalchi et al. [9] and Razus et al. [18]) report the simultaneous effect of elevated temperature and pressure conditions.

The temperature exponent, α values at atmospheric pressure are available, and these values are unavailable at elevated pressure conditions. Similarly, the pressure exponent, β values are available at reference temperature (T_{uo}), and unavailable at elevated temperature conditions. These aspects have been addressed in the present work, and a new modified power-law correlation has been proposed in the present study.

The EHDC method is utilized in this study for the LBV measurement of propane-air mixtures to analyze the simultaneous effect of elevated pressure and temperature conditions. The current measurements are performed at higher mixture pressure (1-5 atm), and temperature (350-630 K) conditions for different mixture conditions (ϕ = 0.7-1.3). The pressure and temperature exponents of the propane-air mixtures are reported using power-law correlation. The mechanism prediction utilizing three comprehensive kinetic models (USC mech II [27], San Diego mech [28], and Qin mech [29]) are compared with the literature and present measurements. The reduction in LBVs with increasing initial pressure is thoroughly investigated. The pressure and temperature exponents from the current work are analyzed with the mechanism predictions and literature data. Lastly, a revised power-law correlation for LBV is suggested, indicating the dependency of β on the temperature ratio, and α on the pressure ratio.

2. Experimental approach

2.1. Experimental arrangement

The schematic diagram of the experimental setup with a pressure vessel (40 Litre) is presented in Fig. 2. A circular toughened glass on the top of the vessel helps to visualize the stabilized planar flame in the diverging channel. The planar flame location within the channel is captured with the help of a digital single-lens reflex (DSLR) camera. The pressure gauge and pressure relief valves are placed on the top plate of the vessel. The ceramic heater is kept 20 mm below the diverging channel, with an axial overlap of 20 mm. The exit plane of the diverging channel holds an ignition device to ignite the premixed propane-air

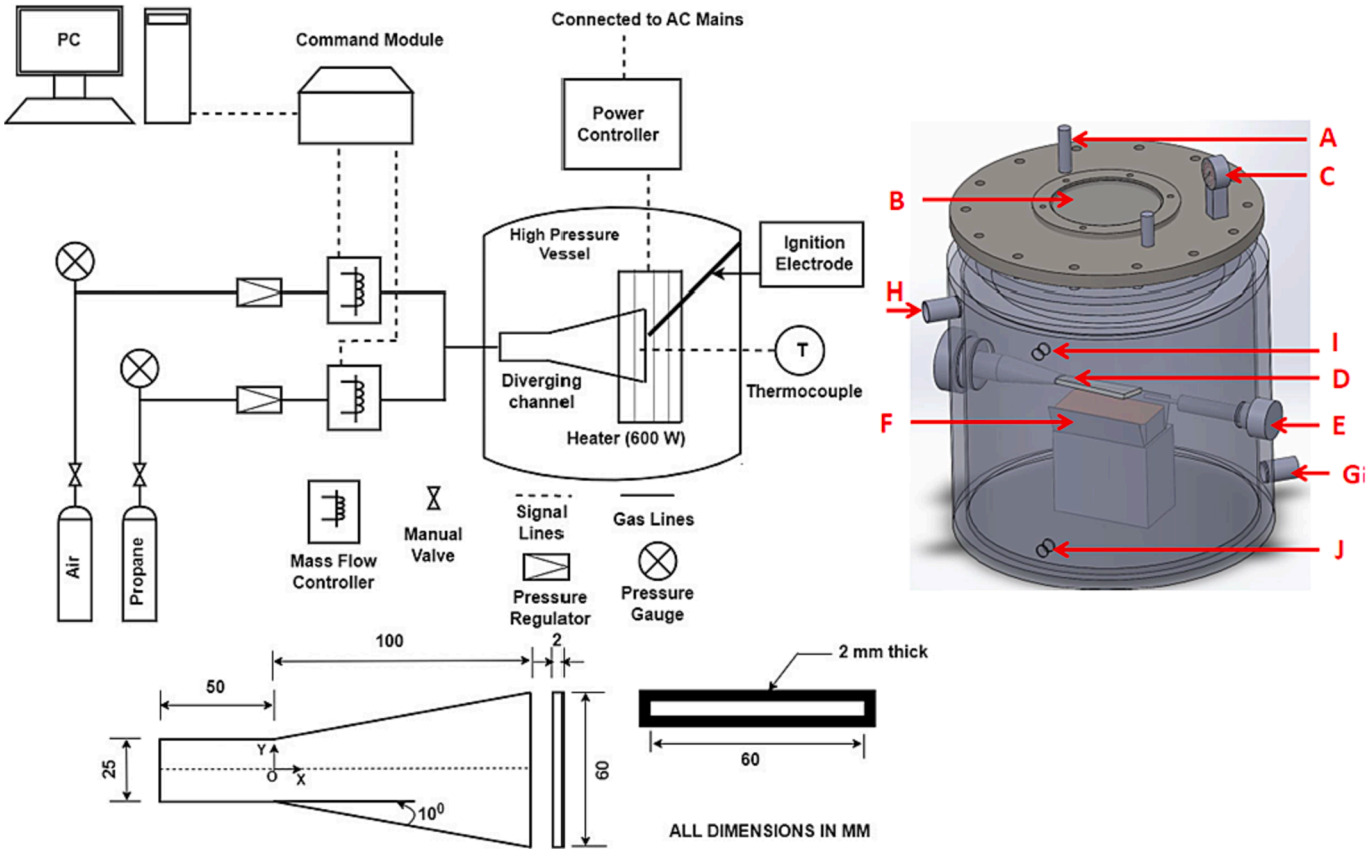

Fig. 2. (a) Layout of the experimental setup, (b) Cylindrical pressure vessel; A – Pressure relief valve, B – Quartz glass window, C – Pressure gauge, D – Diverging channel, E – Thermocouple, F – Ceramic heater, G – Cooling water inlet, H – Cooling water outlet, I and J – Pressurizing Air inlet.

mixture in the pressure vessel. The high-pressure vessel has two air inlets for pressurizing the vessel (one each at the top and bottom). The pressure relief valve regulates the chamber pressure and maintains the same with a precision of ± 0.05 atm of the specified value on the pressure gauge.

The illustrative experimental schematic diagram is shown in Fig. 2a. The diverging channel maintains a uniform temperature and velocity field in the transverse direction, and the divergence aids in the prevention of flame flashback in the channel [30]. A ceramic infrared heater (SHTS/2 Elstein (600 W), Germany) is utilized to heat the diverging channel. As a result, a positive temperature gradient develops in the diverging channel along the mixture flow direction. The exterior heating minimizes the heat loss from the reaction zone to the channel walls, resulting in close to adiabatic conditions along with flame stabilization inside the channel [31]. The positive temperature gradient assists in flame stability and the formation of a planar flame in the channel for various mixture conditions. The cooling water jacket is used to prevent the overheating of the pressure vessel, which enables it to carry out the measurements for a longer experimental duration. Fig. 2b indicates the schematic layout of a pressure vessel. The mixture flow conditions within the channel are precisely regulated by electric mass flow controllers through a command module with a personal computer (PC) interface. The ignition energy delivered by the electrode is insignificant (100-200 mJ) and has no influence on the flow or flame regime within the channel [26]. The premixed fuel-air mixture is supplied at varying pressures depending on the pressure in the high pressure vessel (P_u = 1 - 5 atm). The temperature of the mixture at the channel inlet is 300 K. The mixture temperature is varied between 350-630 K through the use of an external channel heater. The mixture is accurately metered using the electric mass flow controllers and supplied at different mixture equivalence ratios (ϕ = 0.7 - 1.3) and velocities to the channel inlet. This mixture is ignited at the exit of the channel through the ignition system placed within the vessel. The flame gradually propagates through the channel and stabilizes at a location where the mixture flow velocity equals the local burning velocity. A small divergence angle (10^0) of the channel and low air-fuel mixture flow rate result in insignificant hydrodynamic strain in the diverging channel (30-50 s^{-1}) [31]. The direct photograph of stable planar flame is depicted in Fig. 3 at ϕ = 0.7 for the inlet mixture velocity of (U_{in}) 0.6 m/s.

2.2. Temperature measurement and distribution

The measurement of LBV using the EHDC method depends on the unburnt mixture temperature measurements and flame position. Initially, a K-type thermocouple is utilized to assess the air temperature within the channel at different axial locations for cold flow conditions at various flow rates [26]. Thermocouple is operated along the length of the channel using a precise traverse mechanism and measures the temperature of the bottom wall of the channel. For various flow rate conditions, the temperature distribution of the channel is estimated beforehand at different external heating rates. Because the flow Peclet number in the diverging channels (width 2 mm) is low, the unburnt mixture temperature is considered to be close to the inner channel wall temperature at the stabilized flame position [32,33].

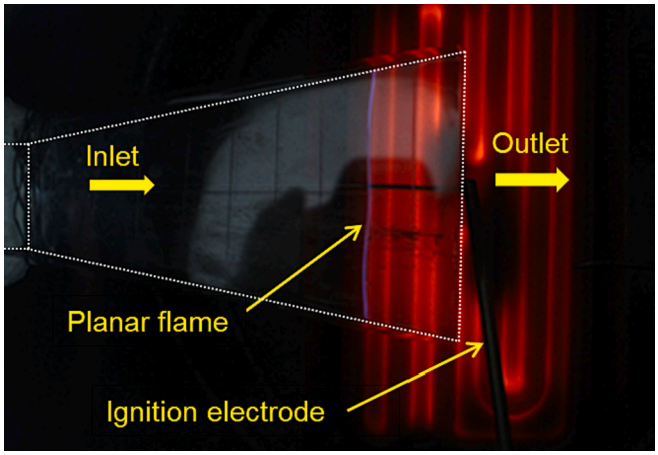

Fig. 3. Stabilized planar flame photograph at ϕ = 0.7 with U_{in} = 0.6 m/s.

The temperature distribution along the channel (cold flow conditions) is shown in Fig. 4 for an external heating rate of 450 W and an intake velocity of U_{in} = 1.1 m/s. A nearly constant temperature profile can be observed in Fig. 4b in the transverse direction, with the highest variation of ± 3 K. For a variety of mixture conditions, this uniform temperature distribution assists in the development of planar flames. For the given conditions, a linear temperature gradient of 4.6 K/mm was noted along the flow direction. From Fig. 4a it can be seen that at a heating rate of 450 W, both the temperature and temperature gradient at 2 atm pressure (4.6 K/mm) is lower than at 1 atm pressure (6.02 K/mm), this is because as pressure increases the unburnt mixture temperature decreases. This necessitates the increasing heating requirements of the channel using an external heater at high pressure conditions.

2.3. Estimation of the mixture burning velocity

The planar flame stabilizes at a position in the diverging channel, where the mixture flow velocity equals the local LBV. The mixture condition (ϕ), inlet mixture velocity, and the channel wall temperature are the different parameters that affect the location of the stabilized flame. The LBV (S_u) in m/s is estimated utilizing the readjusted mass conservation Eqn. (2) as follows [34].

$$S_u = U_{inlet} \times \left(\frac{A_{inlet}}{A_f}\right)\left(\frac{T_u}{T_{in}}\right) \quad (2)$$

where U_{inlet} and A_{inlet} indicate the inlet mixture velocity (m/s) and cross-section area at the inlet of the channel (m^2) respectively, A_f and T_u represent the channel cross-section area and unburnt mixture temperature at the stabilized flame location respectively, and T_{in} represent the unburnt mixture temperature at the inlet of channel.

2.4. Uncertainty study

The flame area, inlet velocity, and mixture temperature all influence the uncertainty of the estimated LBV [31]. The error propagation rule was adopted for estimating the uncertainty of the experimental LBV. The mass flow controllers (AALBORG® GFC17) utilized for air and fuel measurement have uncertainty up to 1.5 % of the full scale reading. The K-type thermocouple employed has a conventional uncertainty of 0.75 % of reading or ± 2.2 K, whichever is greater, influencing the precision of the temperature measurement. The traverse mechanism used for thermocouple movement inside the diverging channel has a ± 1 mm uncertainty, which results in an uncertainty of ± 0.71 mm^2 in the flame area calculation [35]. As per the previous research, the highest level of uncertainty in the estimated burning velocity calculated from this data is anticipated to be less than ± 5 % [31,36]. The least squares method suggested by Alekseev and co-workers [37] was utilized to compute the uncertainty in the pressure exponent (β) and temperature exponent (α). The highest temperature and pressure exponent uncertainty measurement was observed to be $\Delta\alpha = 0.1451$ and $\Delta\beta = 0.052$ respectively. Brief descriptions of the estimation of various uncertainties are given in the supplementary material (section A).

2.5. Modeling study

CHEMKIN-Pro 2020 [38] software is utilized for the computation of 1-D adiabatic premix flames with user specified inlet pressure and temperature conditions. Simulations are performed using different

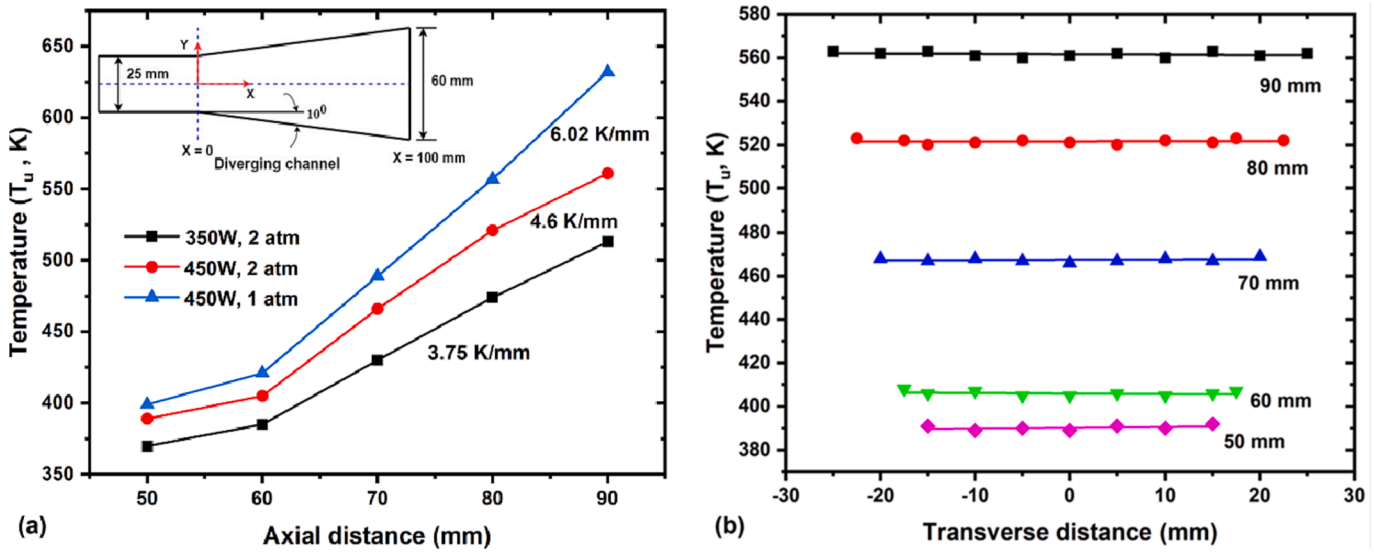

Fig. 4. (a) Temperature distribution in the axial direction for different heating rates (U_{in} = 1.1 m/s, P_u = 1, 2 atm). (b) Temperature distribution in the transverse direction (Q = 450 W, U_{in} = 1.1 m/s, P_u = 2 atm).

kinetic models viz. USC mech II [27], San Diego mech [28], and Qin mech [29] with a maximum number of grid points of 2000 along the axial length of the domain. The adaptive mesh parameters values of GRAD and CURV are set as 0.03 and 0.04 respectively, to get almost zero temperature slopes at the boundaries.

3. Results and discussion

3.1. LBV at higher mixture temperature (P_u = 2 atm)

LBV (S_u) variation with temperature ratio (T_u/T_{u0}) for propane-air mixtures is shown in Fig. 5. Symbols represent the measured data, and the lines indicate different kinetic model predictions. The measured data are plotted using the power-law correlation, $S_u = S_{u0} \times (T_u/T_{u0})^{\alpha}$, where T_{u0} is the reference temperature of 300 K, T_u is the unburnt mixture temperature, α is the temperature exponent, and S_{u0} is LBV at a reference temperature. It is obvious from the plot that LBV enhances with a rise in unburnt mixture temperature, as a consequence of the elevated enthalpy content, and higher adiabatic flame temperature of the fuel-air mixture. Discrepancies in the kinetic variables (due to variation in the reaction rate constants, reaction activation energies, and third body efficiencies) and the exclusion and inclusion of specific species and different reactions in these comprehensive kinetic mechanisms is the major cause in the variation of the LBV predictions from different kinetic models. It is clear from Fig. 5 that the current results are close to the mechanism predictions of San Diego mech [28] for the entire temperature ratio range. At ϕ = 1, S_{u0} = 31.42 cm/s and α = 1.87 are observed as per current measurements for P_u = 2 atm. The equation and the power-law fit parameters are indicated in the inset table. Similar equations are obtained for different mixture conditions (ϕ), and high pressures (P_u = 1-5 atm), helping in evaluating the temperature exponents (α), and LBV (S_{u0}) at reference conditions (300 K). Fig. 5 also depicts a reduction in the LBV due to a rise in the mixture pressure (1 to 2 atm) at stoichiometric mixture conditions.

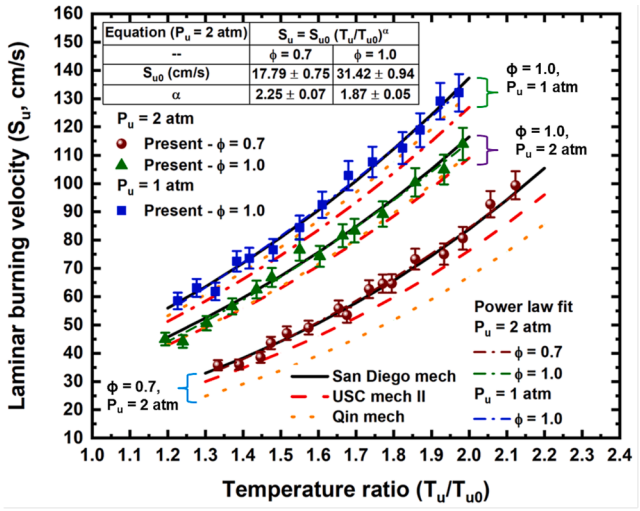

Fig. 5. Variation of LBV for the propane-air mixture at higher temperatures and P_u = 1, 2 atm for ϕ = 0.7 and 1.0.

3.2. LBV variation at different pressures

In Fig. 6a, the present measured LBV is compared with the kinetic model predictions, such as USC mech II [27], San Diego mech [28], and Qin mech [29], along with earlier studies [10,21–23] at 300 K for different mixture conditions (ϕ = 0.7-1.3) at different pressure of 1, 2 and 4 atm. The present results are close to the San Diego mech [28] mechanism predictions from lean to the stoichiometric mixtures, and slightly over predict for rich mixture conditions. However, the maximum deviation between the present results and kinetic model predictions (~9 %) is noticed at ϕ = 1.1 at 4 atm pressure conditions. The current results match well with the literature data for the entire mixture range at 1 atm within the uncertainty limits. The experimental results of Jomaas et al. [21], and Goswami et al. [23] show lower LBV for lean mixture conditions, and higher LBV values for rich mixture conditions at 2 atm, while at 4 atm pressure, it matches at ϕ = 0.9 and 1.0 with Goswami et al. [23] within an uncertainty limit of ± 5 %. Fig. 6b indicates a similar comparison of present results at 3, and 5 atm with the predictions of the San Diego mech [28] mechanism (maximum deviation ~ 12 % at ϕ = 1.1 for 5 atm pressure condition). The current results are a better match with the measurements of Hassan et al. [10] at ϕ = 0.9-1.1 and 1.3 (3 atm pressure), while at 5 atm pressure, it matches well with the measurements of Jomaas et al. [21] at the majority of the mixture conditions within the uncertainty limit. Fig. 6a and 6b indicate the observation of a significant reduction in the LBV values with an increment in the mixture pressure.

The overall mixture pressure dependence of LBV can be demon-

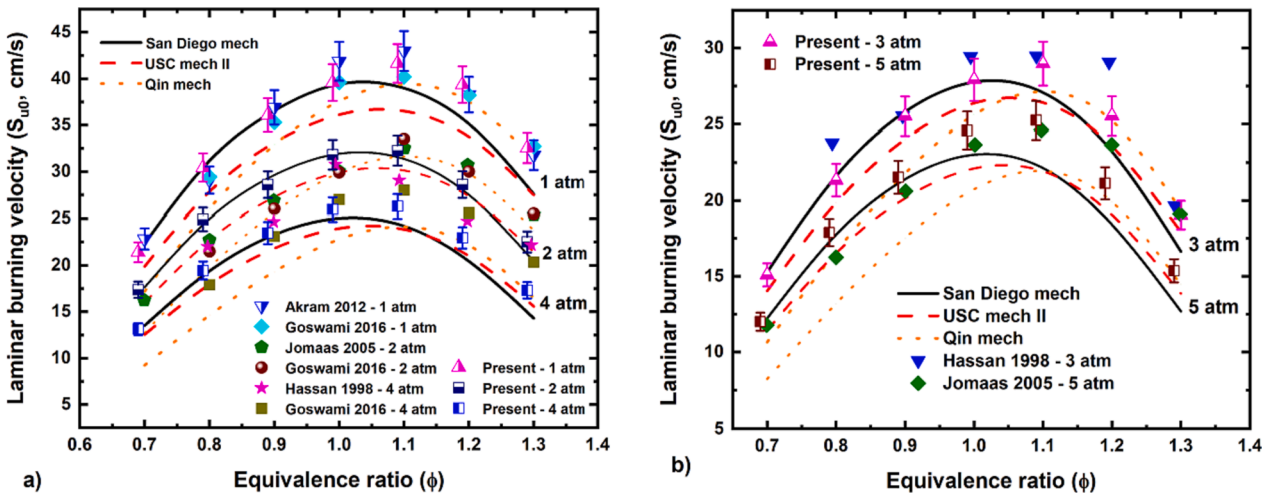

Fig. 6. LBV of the propane-air mixture at different pressures (a) 1, 2, 4 atm, and (b) 3, 5 atm and reference temperature (300 K) with mechanism predictions (lines) and literature measurements using other techniques (symbols).

strated in the form,

$$S_u = S_{u0}\left(\frac{p_u}{p_{uo}}\right)^{\beta} \tag{3}$$

Where S_{u0} is the LBV at reference condition (p_{uo} = 1 atm) and, β - pressure exponent. The pressure exponent, β, is a function of mixture conditions (ϕ) and the range of mixture pressures. From the comprehensive and thermal theories of LBV analysis, the dependency of LBV on pressure can be demonstrated as , $S_u \propto p^{(n-2)/2}$, where n represents the overall reaction order. For majority hydrocarbon-air mixtures, the overall reaction order is reported to be less than 2 with S_u less than 50 cm/s, suggesting that the LBV reduces with the rise in mixture pressure [39]. As a result, the reported pressure exponent, β is observed to be negative for hydrocarbon-air mixtures. The LBV decreases as pressure increases owing to the density variation in the mixture. The decrease in the mean free path caused by the increase in mixture density results in molecular collisions, which raises the collision frequency. This results in higher third-body recombination reactions and also increased third-body effects. At higher pressures, the reaction zone thickness gets reduced as well. At elevated pressures, the oxidation rate is also affected due to the thermal diffusivity of the mixtures [26].

3.3. Temperature exponent variation at higher pressures

The temperature exponent (α), an empirical parameter that indicates a rise in LBV at elevated temperatures, was deduced from power-law correlations for the measured LBV data, at given pressure conditions for the mixture range (ϕ = 0.7-1.3). Fig. 7 depicts the comparison of the estimated temperature exponent data with the mechanism predictions of San Diego mech [28], at different pressures (P_u = 1-5 atm). The current results are slightly offset on the x-axis (P_u = 4 and 5 atm) to avoid the overlapping of the data for better understanding. The pressure effect on the temperature exponents is investigated and reported. The temperature exponent exhibits non-monotonic behavior with mixture conditions and it is noted to be minimum at slightly rich mixture conditions for the entire pressure range (1-5 atm). For the range of equivalence ratio, the temperature exponents were found to rise slightly with increasing pressure. The temperature exponents deduced from the measurements agree well with the mechanism predictions of San Diego mech [28] within the uncertainty limit, and specifically, it matches well from lean to stoichiometric mixture conditions for the entire pressure range (P_u = 1-5 atm). The measured data of Akram et al. [22] are observed to be lower than the current results for the entire mixture range at 1 atm. This is perhaps due to the high temperature range and increased number of data points obtained in the current work as demonstrated by Varghese

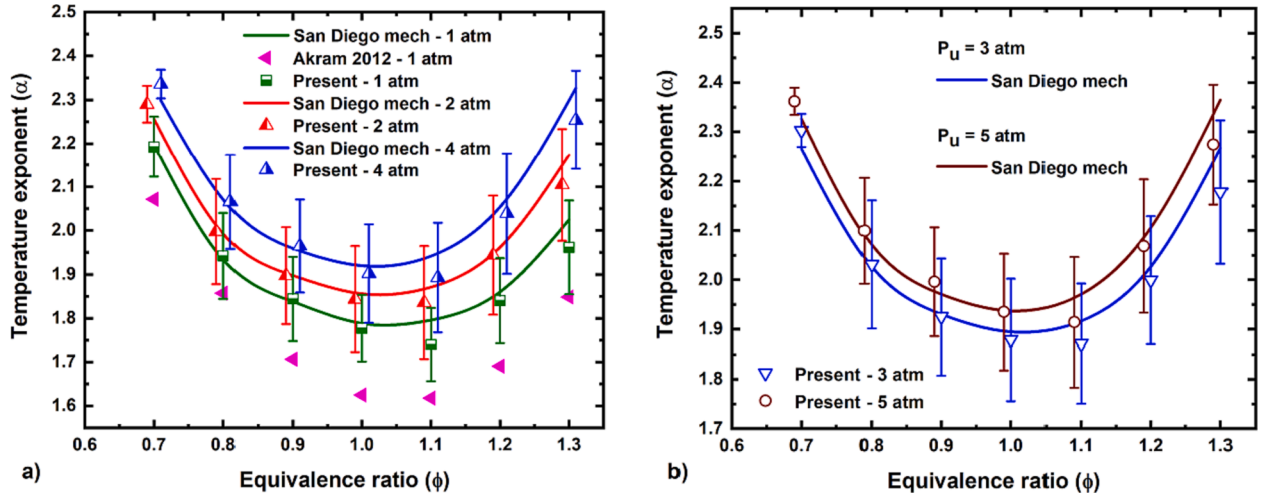

Fig. 7. Temperature exponents (α) variation for the propane-air mixture at different pressures (a) P_u = 1, 2, 4 atm and (b) P_u = 3, 5 atm.

et al. [26] for premixed methane-air mixtures. The pressure dependency of the temperature exponents is visible in Fig. 7, and it can be demonstrated that it is linear for stoichiometric mixtures [40]. With increasing pressure, a slight increase in the temperature exponent was noticed, and the temperature exponent variation for the stoichiometric propane-air mixture can be obtained as $\alpha = 1.75 + 0.037\ (P_u/P_{u0})$.

3.4. LBV variation at higher temperatures and pressures

Fig. 8 depicts the LBV variation for different pressures (P_u = 1-5 atm), and at a higher temperature of $T_u = 600$ K with a mixture range, ϕ = 0.7-1.3. The Temperature exponent values (α) obtained earlier, were used in power-law correlations to obtain the current measurements for all mixture and pressure conditions. For the majority of mixture conditions (ϕ) at all pressures, the current results are broadly in line with the mechanism predictions of San Diego mech [28]. Fig. 8a indicates that the mechanism predictions of San Diego mech [28] are closer to the current measurements for lean to stoichiometric, and it under predicts for rich mixture conditions, this is perhaps due to higher values of S_{u0} observed in the current measurements. The measured data of Wang et al. [20] are reported to be lower than the current results and kinetic model predictions at $\phi = 0.7$, and 0.8 based on the correlations reported in their literature. The measurements of Akram et al. [22] are observed to be marginally lower than the present results for the entire mixture range at 1 atm. It is because of the lower values of temperature exponent noted in their work. A similar trend is observed in Fig. 8b, with a maximum deviation of ~ 11 % at $\phi = 1.1$ for 5 atm pressure conditions. In general, an increase in the unburnt gas temperature enhances the LBV of any fuel-air mixture for all equivalence ratios, owing to its higher enthalpy content, and a higher concentration of radical species (O, H, OH, and CH_3) at higher mixture temperatures. The rise in these radical species, combined with elevated adiabatic flame temperatures, presents a rapid rate of heat release. The higher enthalpy of the unburnt mixture enhances the LBV. With increasing pressure, the LBV decreases at a specific mixture condition and unburned gas temperature. For example, the subsequent empirical equation can be stated to demonstrate the LBV variation at various higher pressures and temperatures under stoichiometric mixture conditions.

$$S_u = 39.6\left(\frac{T_u}{T_{u0}}\right)^{\propto}\left(\frac{P_u}{P_{u0}}\right)^{\beta};$$
$$\propto = 1.75 + 0.037\frac{P_u}{P_{u0}};\ \beta = 0.065\frac{T_u}{T_{u0}} - 0.361 \quad (4)$$

According to the measured LBVs, the current work suggests the pressure exponent as a function of the temperature ratio and the temperature exponent as a function of the pressure ratio. For different mixture conditions (ϕ), a linear increase in pressure and temperature exponent was observed. Fig. 8 indicates the temperature and pressure exponent variation as a function of the pressure ratio and temperature ratio respectively for the entire mixture range (ϕ = 0.7-1.3) owing to their linear dependency on each other. Fig. 9a depicts the temperature exponent (α) variation of propane-air mixtures at higher pressures for different mixture conditions. With increasing pressure, the temperature exponent increases linearly. As indicated in Fig. 9a, the temperature exponents are compared with the mechanism predictions of the San Diego mech. The current results are in good match with the mechanism predictions at stoichiometric mixture conditions. However, at lean mixture conditions, mechanism predictions under predict with present results for the entire pressure range (except at $P_u = 1$ atm), and at rich mixture conditions, the kinetic model consistently over predicts for the entire pressure range with maximum deviation ~ 4 % at $P_u = 1$ and 5 atm. Fig. 9b indicates the pressure exponent (β) variation with temperature ratio for different mixture conditions similar to Fig. 9a. The linear fit slope of the temperature exponents at various pressures is remarkably lower as compared to the slopes of Fig. 9b, suggesting a major temperature dependency of pressure exponents, as compared to the pressure dependency of temperature exponents. The pressure exponents, β, predicted by the San Diego mech [28] mechanism varies from the current measurements. As seen from Fig. 9b, the over predictions of the mechanism are observed with present results for all mixture conditions over an entire temperature range. Fig. 9 clearly shows that it is important to take into consideration the pressure and temperature variation, when expressing the temperature and pressure exponents (α, β) as functions of pressure ratio and temperature ratio, respectively, instead of the constant (α, β) values proposed earlier by various researchers [9,11,18,23] in the conventional power-law correlations. A revised power-law correlation is suggested from current experimental measurements by considering the variation in α and β as

$$S_u = S_{u0}\left(\frac{T_u}{T_{u0}}\right)^{\propto_0+\propto_1\left(1-\frac{P_u}{P_{u0}}\right)}\left(\frac{P_u}{P_{u0}}\right)^{\beta_0+\beta_1\left(1-\frac{T_u}{T_{u0}}\right)} \quad (5)$$

where α_i and β_i are the linear fit's coefficients deduced from Fig. 9. The Supplementary material (section B) includes an entire list of the linear fit coefficients, along with the LBV values (S_{u0}) at ambient conditions (T_{u0} = 300 K, P_u = 1 atm) as shown in Tables 6 and 9.

3.5. Pressure exponent variation with the mixture conditions (ϕ)

A higher mixture pressure reduces the flame propagation rate of

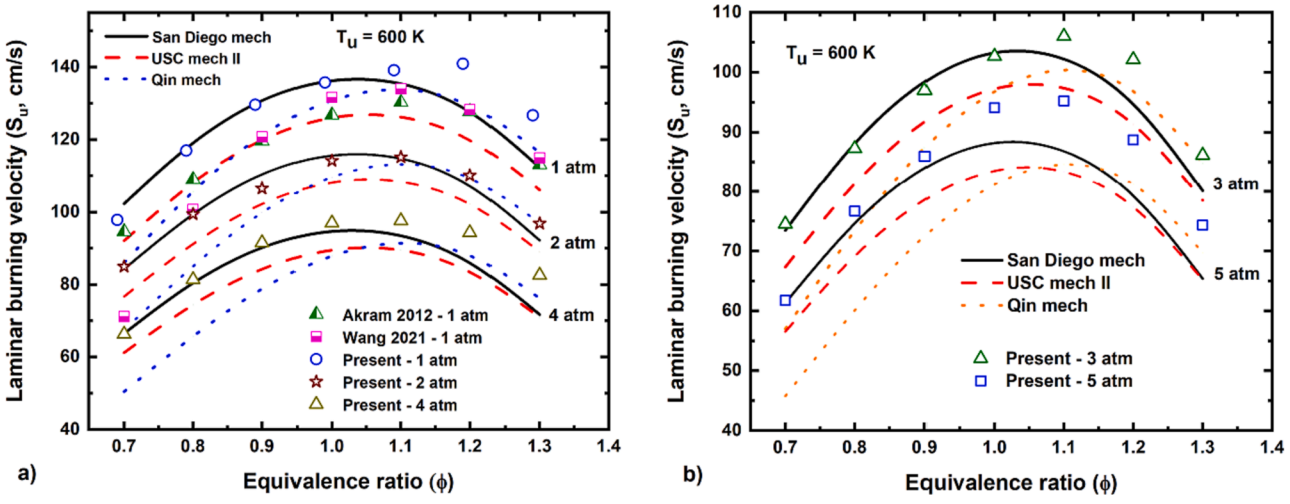

Fig. 8. Variation of LBV at different pressures [a] P_u = 1, 2, 4 atm and [b] P_u = 3, 5 atm with mixture temperature T_u = 600 K.

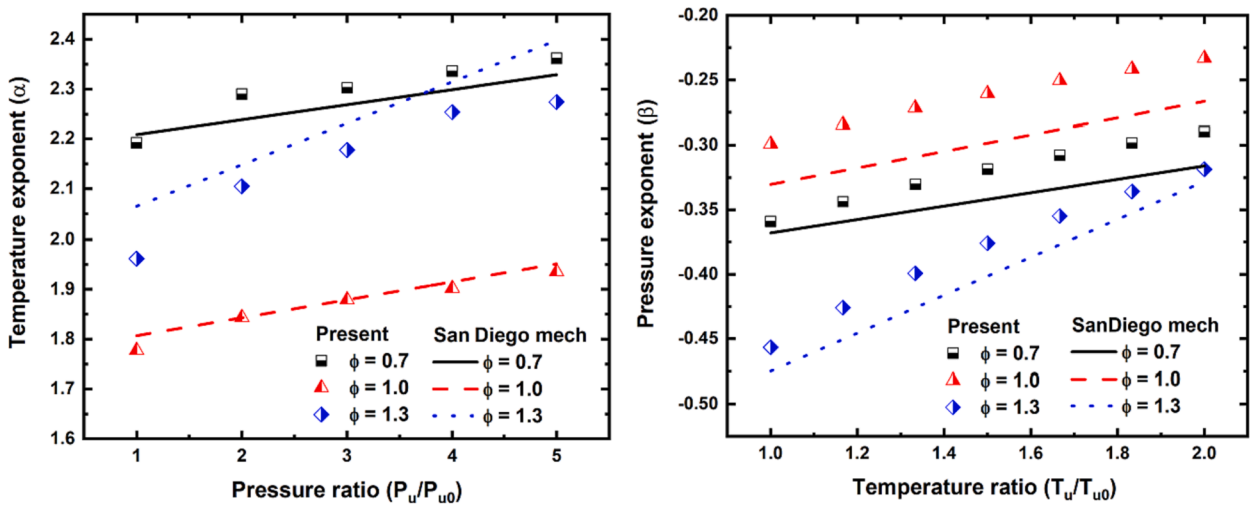

Fig. 9. (a) Temperature exponent (α) comparison at various pressure ratios and (b) pressure exponent (β) comparison at various temperature ratios of a propane-air mixture.

propane-air mixtures through different routes, lowering the mixture LBV. Chemical kinetics is the major route of the influence of the mixture pressure on flame propagation. It accounts for a vital role in lowering the mixture LBV with mixture pressure. The LBV is influenced due to a variation in the mixture thermophysical properties (higher density, thermal diffusivity) as well as the corresponding variation in the collision frequency of the third body reactions. The rise in initial pressure has a secondary effect on the transport and thermodynamic properties of the mixture [26]. Fig. 10 depicts the LBV (S_{u0}) variation of C_3H_8-air mixtures at different mixture conditions and their decrement with a rise in pressure. The power-law pressure dependence, $S_u = S_{u0}\left(\frac{P_u}{P_{u0}}\right)^{\beta}$, is deduced from the slope of these straight lines on a logarithmic scale as shown in Fig. 10, it also indicates a comparison at ϕ = 0.8, 1.0, and 1.3 with the measured data of Goswami et al. [23]. It is evident from Fig. 10 that the current results are a better match with the measurements of Goswami et al. [23] at ϕ = 1.0. Whereas higher values of the present measurements at ϕ = 0.8 and lower values at 1.3 (except at P_u = 1 atm) are observed compared to the measured data of Goswami et al. [23].

Fig. 11 compares the pressure exponent values β, deduced from Fig. 10, with the similar measurements available in the literature. The pressure exponent exhibits a non-monotonic behavior, with the occurrence of the maximum value of β at ϕ = 1.0. Fig. 10a indicates that the current results match well with the kinetic model predictions of USC mech II [27] at ϕ = 0.8-1.1, and a better match with the mechanism predictions (San Diego mech and USC mech II) within the uncertainty limits. The measured data of Goswami et al. [23] are in good match with the current results at ϕ = 0.8-1.0, and higher values at ϕ = 1.1-1.3. The pressure exponents from various literature data [9,11,18,23] are compared with the current measurements. A significant scatter is observed in Fig. 11a, and this is owing to various measurements and data extraction methods adopted by various researchers. Fig. 11b depicts the variation of the pressure exponent (β) at higher temperatures (T_u = 600 K). A marginal difference in current measurements and kinetic model predictions is observed in ϕ = 0.7-1.1 range. This is perhaps due to the variation in the LBV at reference conditions (S_{u0}) and temperature exponent (α), at different pressure conditions (P_u = 1-5 atm) in comparison to the various mechanism predictions. A maximum deviation of ~ 7 % at ϕ = 1.0 is noted between present measurements and kinetic model predictions.

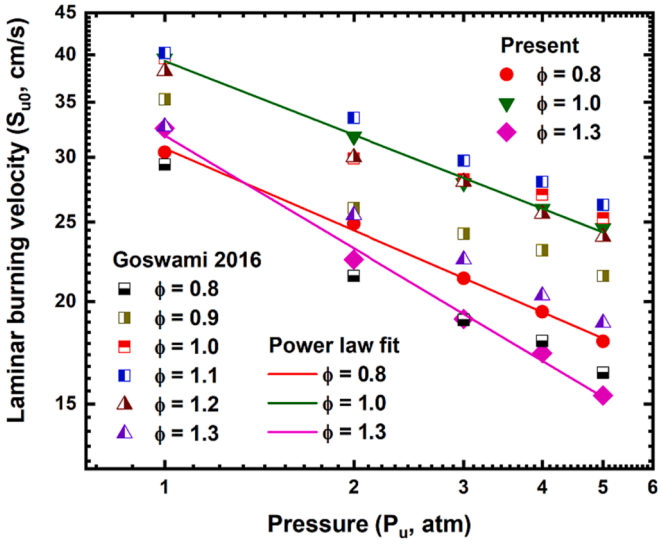

Fig. 10. LBV of propane-air mixtures for different mixture conditions and higher pressures at reference temperature (300 K).

3.6. Sensitivity analysis

Sensitivity coefficients are used to determine which reactions and species have the highest influence on the variation of LBV. The results of sensitivity analysis are very useful and helpful to refine the detailed kinetic models by removing or modifying the reactions or species with low sensitivity coefficients, or adding new reactions or species that have a high influence on the LBV. Eqn. (6) defines the normalized sensitivity coefficient for the LBV as the fractional change in the mixture burning velocity $S_{u,i}$ brought on by a fractional change in the rate of a specific reaction k_j [41].

$$Sens(S_u, k) = \frac{\partial log S_{u,i}}{\partial log k_j} = \frac{k_j}{S_{u,i}}\left(\frac{\partial S_{u,i}}{\partial k_j}\right) \quad (6)$$

where k_j is the reaction rate of reaction j and $S_{u,i}$ is the laminar burning velocity of species i.

At different mixture conditions (ϕ = 0.8, 1.0, and 1.2), temperature (300 and 600 K), and pressure (1 and 5 atm), the sensitivity analysis of significant reactions from the San Diego mech [28] mechanism has been examined for propane-air mixtures.

Out of 268 reactions, Fig. 12a and b depict the impact of 15 important elementary reactions on the LBV under various mixture conditions of 1 atm, 300 K, and 5 atm, 600 K respectively. The LBV enhances due to elementary reaction, which has positive values of normalized sensitivity

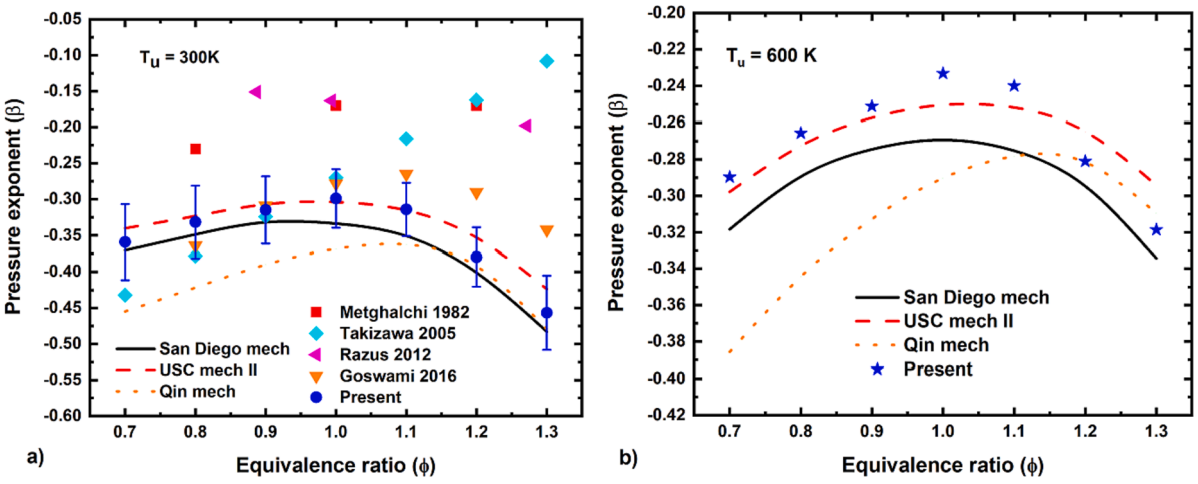

Fig. 11. Pressure exponent comparison at various mixture conditions (ϕ) with the literature and mechanism predictions ([a] T_u = 300 K [b] T_u = 600 K).

coefficient, and vice-versa for the elementary reactions with negative values of sensitivity coefficient. It can be observed that reactions involving H radicals were the most sensitive ones, and their sensitivity increased with an increase in pressure and temperature at all mixture conditions. With an increase in pressure and temperature, the magnitude of most of the sensitivity coefficients of elementary reactions increases, whereas some reactions become active and inactive due to a rise in the overall reactivity and rate of consumption of radicals. Among all the reactions, the chain branching reaction H + O_2 ↔ OH + O (R1), has the most positive sensitivity coefficient at all the mixture conditions, pressure, and temperature. The primary CO oxidation reaction, CO + OH ↔ CO_2 + H (R25), generates heat and an H radical, which enhances reaction R1. Along with R25, the decomposition of formyl radical (HCO) through the reaction HCO + M ↔ CO + H + M (R28), is a significant source of H-atoms for the premixed propane-air mixtures. Reactions R10 and R222 become inactive with a simultaneous increase in mixture pressure and temperature, whereas reactions R48 and R219 become active at rich (ϕ = 1.2) and lean (ϕ = 0.8) mixture conditions respectively. Nearly 45% increase in negative sensitivity is observed at all mixture conditions for the chain termination reaction H + CH_3 (+M) ↔ CH_4 (+M) (R56), due to enhancement in the recombination of H radical and third body effects with a rise in pressure and temperature from 1 atm, 300 K to 5 atm, 600 K. A maximum decrement in the positive sensitivity is observed at all mixture conditions for the reaction HCO + M ↔ CO + H + M (R28), due to an increase in the third body effects with pressure and temperature.

3.7. Reaction pathway analysis

The generation and utilization of major and minor species associated with a complicated kinetic model are graphically represented in a reaction pathway diagram. Reaction path analysis enables the identification of slow reactions and species with low net production rates, which are thought to be unimportant and can be safely eliminated from the entire mechanism. This information can be used to design a simplified mechanism [42]. The relative significance of a given reaction path is shown by the thickness of the arrow lines and different color gradients. The numerical values that appear to the right of arrowed lines express how quickly the reactant is destroyed or formed. The following Eqn. (7) calculates the elemental flux of element A through reaction step i from species j to species k [43].

$$A_{ijk} = \frac{n_{A,j} n_{A,k} r_i}{N_{A,i}} \tag{7}$$

where, $n_{A,j}$ and $n_{A,k}$ are the number of atoms A in species j and k, respectively, and $N_{A,i}$ is the sum of the number of atoms A on either side of reaction step i in all species, whilst r_i is the rate of reaction step i. The sum of all elemental fluxes at a certain reaction time is used to determine the total elemental flux, which also accounts for any potential reaction steps that could change species j into species k.

The reaction pathway diagrams of the propane-air mixture at stoichiometric conditions and unburnt mixture pressure and temperature conditions of 1 atm, 300 K and 5 atm, 600 K are shown in Figs. 13 and 14 respectively to show the simultaneous effect of temperature and pressure. A Graphviz [44] dot tool utilizing the San Diego mech [28] mechanism and Cantera [45] coupled with Python programming [46] was used to estimate the reaction route for the elemental flux of carbon. The threshold value of the flux is set as 0.03 of the largest flux and all fluxes that are smaller than 3 % of the largest flux are removed. The threshold setting helps the reaction pathway diagram to get rid of any unnecessary paths. Out of all the species, 22 major species play significant roles in the reaction pathway diagram and related paths with their elemental flux values are indicated in Figs. 13 and 14 respectively. As the pressure and temperature are increased from 1 atm, 300 K (Fig. 13) to 5 atm, 600 K (Fig. 14) there is considerable change in reaction paths and associated elemental flux.

The oxidation of propane proceeds with the formation of isopropyl radical and n-propyl radical. The detailed reaction pathway diagram at an initial temperature of 300 K and pressure of 1 atm is shown in the supplementary material (section C), for the reactor temperature of 1100 K. The threshold elemental flux is set as 0.003 kmol/m^3-s. For the same mixture temperature and pressure condition, when the reactor temperature is increased to 1650 K, the elemental flux associated with the reactions in the formation of ethene (C_3H_6) species from propane gets reduced as shown in the supplementary material (section C).

Maximum increment in elemental flux is observed from 0.0435 (at 300 K, 1 atm) to 0.176 (at 600 K, 5 atm) (highlighted in Figs. 13 and 14 by green color) by 305 % when ethane (C_2H_6) is formed from its predecessor methyl radical (CH_3) through reaction R57: CH_3 (+M) C_2H_6 (+M). This increase in elemental flux between the species of ethane and methyl radical activates the CH_3 → C_2H_6 → C_2H_5 → C_2H_4 pathway.

Maximum reduction in the elemental flux is observed for the reaction between the species carbon monoxide (CO) and carbon dioxide (CO_2) by 61% (highlighted in Figs. 13 and 14 using red color) through following reactions R24: CO + O (+M) ⇔ CO_2 (+M), R25: CO + OH ⇔ CO_2 + H, R26: CO + HO_2 ⇔ CO_2 + OH, R27: CO + O_2 ⇔ CO_2 + O, R60: S-CH_2 + CO_2 ⇔ CO + CH_2O, R73: CH + CO_2 ⇔ HCO + CO, R189: CH_3CH_2O + CO ⇔ C_2H_5 + CO_2. As the temperature and pressure are varied from 300 K, 1 atm to 600 K, 5 atm, methane (CH_4) species become inactive and do not participate in the reaction pathway diagram, whereas there is a negligible effect (1.09 %) on the elemental flux for the path taken by species HCO to form CO_2. With a rise in temperature and pressure to 600

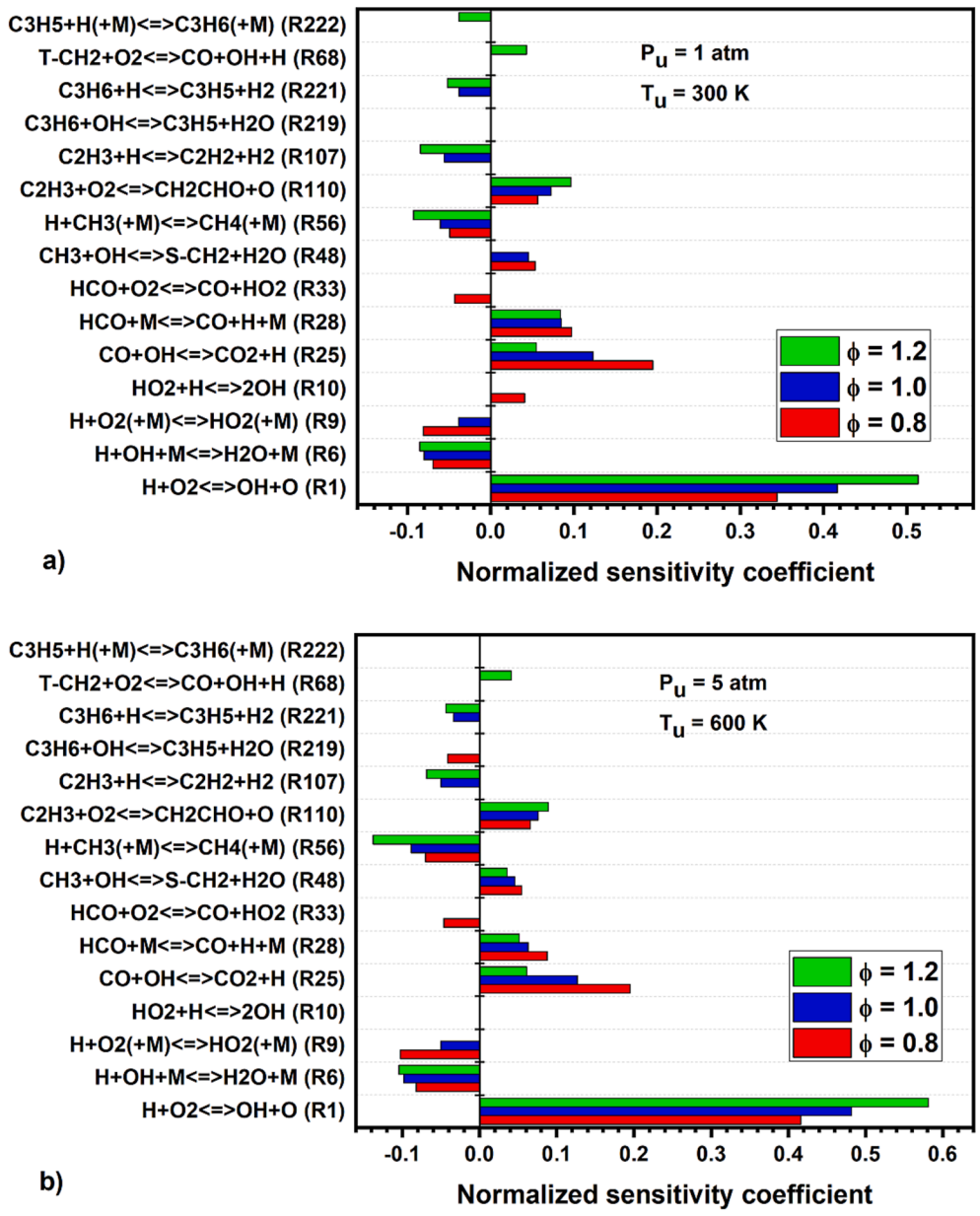

Fig. 12. Normalized sensitivity analysis of propane-air mixture at (a) 300 K, 1 atm and (b) 600 K, 5 atm.

K, 5 atm, many reactions show higher elemental flux and some of them show lower values of elemental flux compared to the values of elemental flux at 300 K, 1 atm conditions indicating a change in the reaction pathway diagram owing to the simultaneous effect of temperature and pressure. Few reactions become active and participate in the reaction pathway diagram with an increase in pressure and temperature as highlighted in Fig. 14 using magenta color.

4. Conclusions

The current study reports the LBV measurements for propane-air mixtures utilizing the EHDC method. The current measurements are conducted at higher unburnt mixture temperatures (350-630 K), and pressures (1-5 atm) over the mixture range ($\phi = 0.7$-1.3). This method is used to minimize the heat losses and obtain unstretched planar flames to measure the LBV at given conditions. The properties of the stabilized planar flames are used to evaluate the LBV and to obtain the temperature and pressure exponents from the current measurements. The major key findings of the current work are as follows:

- The LBV of the propane-air mixture is found to increase with the unburnt mixture temperature, for all equivalence ratios at all pressure conditions.
- The present measurement agrees well with the mechanism predictions of San Diego mech at most mixture conditions.
- The parabolic trend was observed for the LBV variation with the mixture conditions (ϕ), along with the maxima at $\phi = 1.1$.
- The present experimental LBV measurements are in good match with the existing measurements observed in the literature using various techniques.
- The LBV is observed to decrease with an increase in the mixture pressure.
- The inverted parabolic variation of temperature exponent (α) with equivalence ratio (ϕ) was noted, along with minima at $\phi = 1.1$. The pressure exponent (β) variation with the mixture conditions (ϕ) is similar to the LBV, along with maxima at $\phi = 1.0$.
- The temperature exponent increases linearly with the pressure ratio, and a similar trend is observed for the pressure exponent with the mixture temperature ratio.

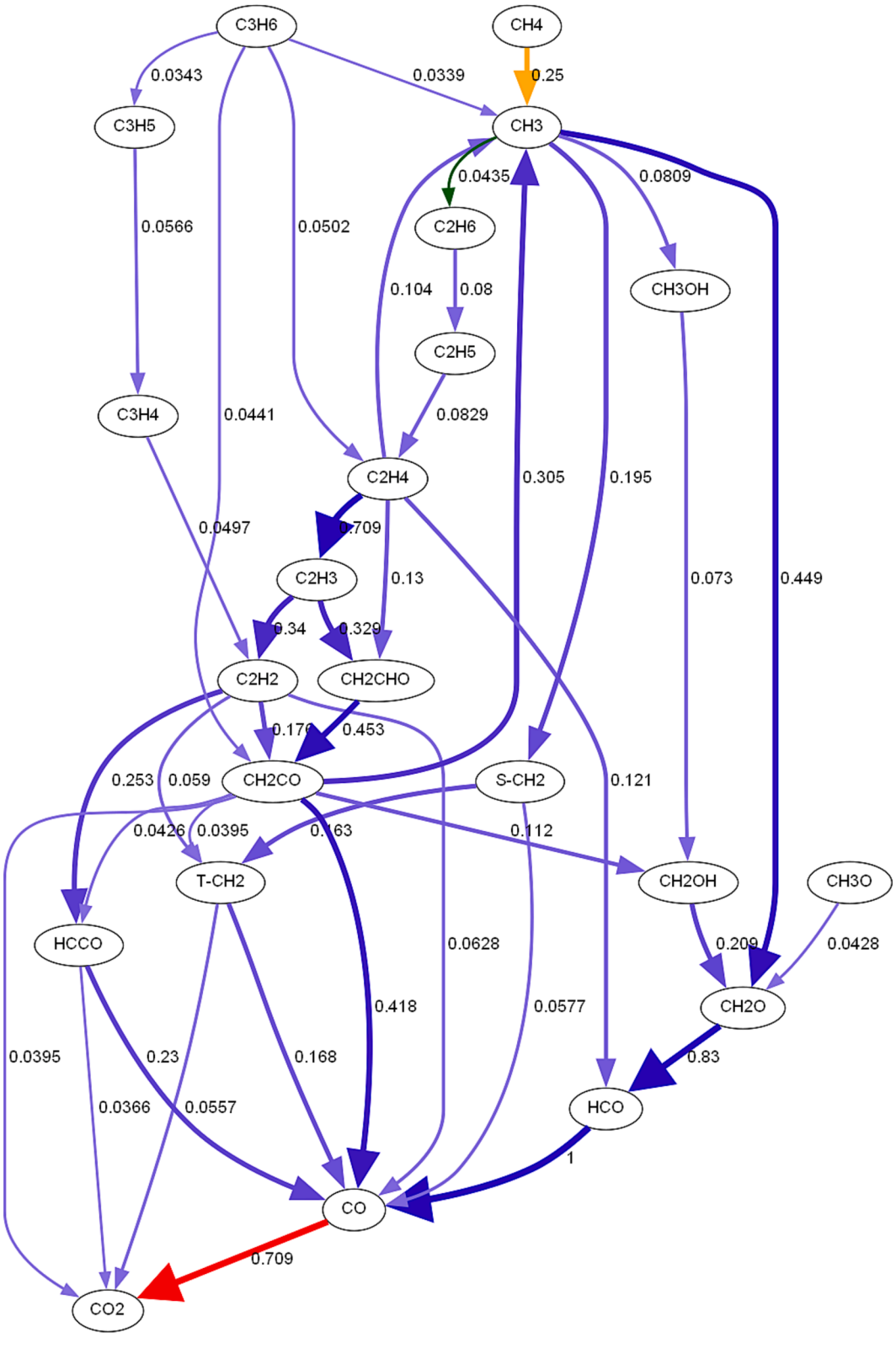

Fig. 13. Reaction pathway diagram of propane-air mixture for the stoichiometric mixture condition at 300 K and 1 atm.

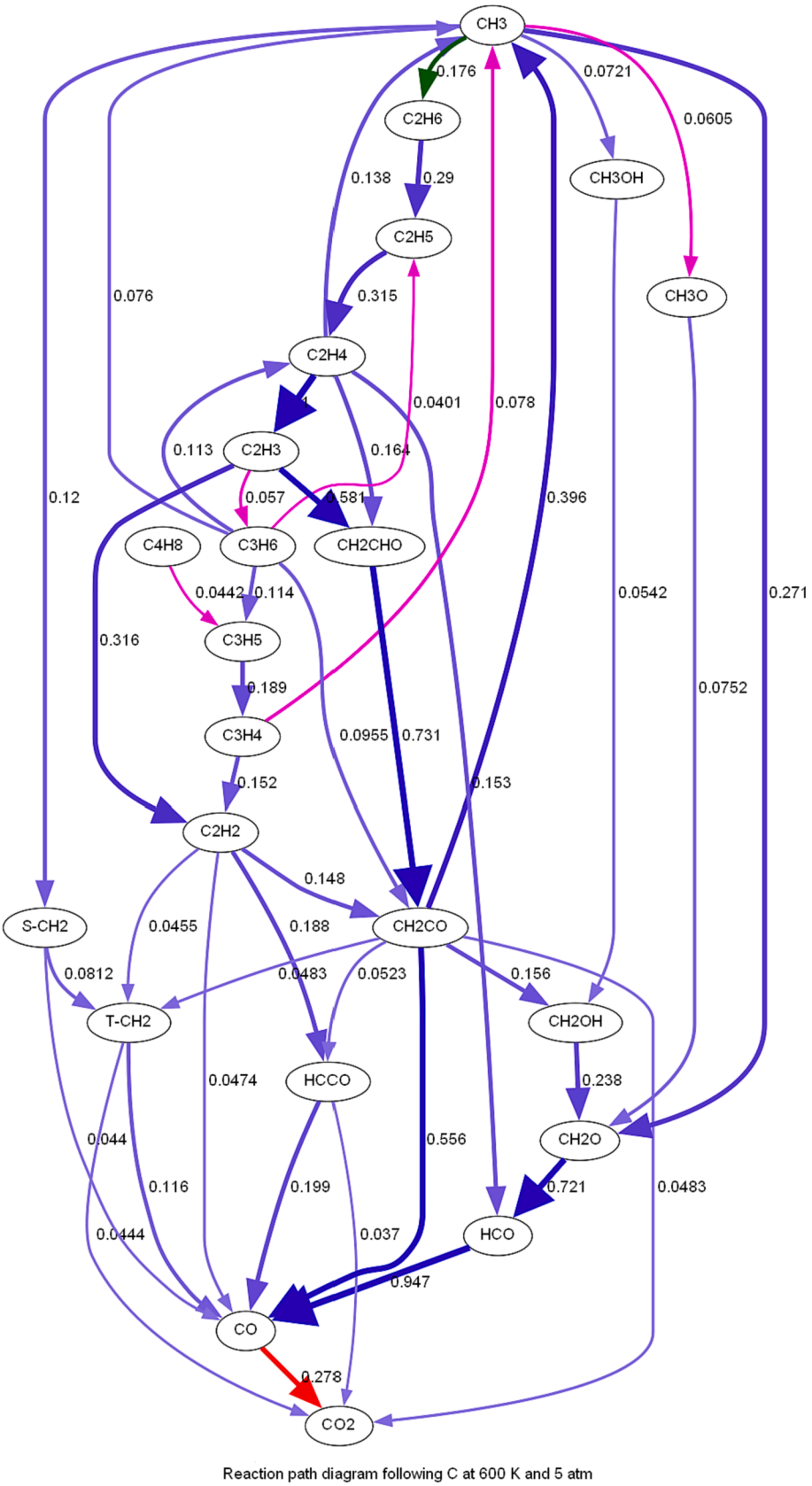

Fig. 14. Reaction pathway diagram of propane-air mixture for the stoichiometric mixture condition at 600 K and 5 atm.

- The current study suggested a revised power-law correlation, indicating a new form for temperature exponent as a linear function of pressure ratio and pressure exponent as a function of temperature ratio, as $S_u = S_{u0}\left(\frac{T_u}{T_{u0}}\right)^{\propto_0+\propto_1\left(1-\frac{P_u}{P_{u0}}\right)}\left(\frac{P_u}{P_{u0}}\right)^{\beta_0+\beta_1\left(1-\frac{T_u}{T_{u0}}\right)}$
- A significant increase (≈ 45%) in negative sensitivity is observed at all mixture conditions for the chain termination reaction H + CH_3 (+M) ↔ CH_4 (+M) (R56), due to an enhancement in the recombination of H radical and third body effects with an increase in pressure and temperature from 1 atm, 300 K to 5 atm, 600 K. However, the maximum decrement in positive sensitivity is observed at all mixture conditions for the reaction HCO + M ↔ CO + H + M (R28), due to an increase in the third body effects with pressure and temperature.
- The reaction pathway analysis reveals, a maximum increment in elemental flux from 0.0435 (at 300 K, 1 atm) to 0.176 (at 600 K, 5 atm) by 305 %, when ethane (C_2H_6) is formed from its predecessor methyl radical (CH_3) through reaction R57: CH_3 (+M) ⇔ C_2H_6 (+M). A maximum reduction in elemental flux is observed for the reaction between the species carbon monoxide (CO) and carbon dioxide (CO_2) by 61% through various reactions.

Declaration of Competing Interest

The authors declare that they have no known competing financial interests or personal relationships that could have appeared to influence the work reported in this paper.

Data availability

Data will be made available on request.

Acknowledgement

This work was funded by Science and Engineering Research Board India, SERB (Project number CRG/2020/001700). Vijay Shinde is grateful to his parent institute K. J. Somaiya College of Engineering, Mumbai for sponsoring to pursue doctoral program at IIT Bombay, and also to Mr. Jitendra Kumar for his sincere support and assistance during experimental measurements.

Appendix A. Supplementary material

Supplementary data to this article can be found online at https://doi.org/10.1016/j.fuel.2023.129561.

References

[1] Mardi KM, Khalilarya S, Nemati A. A numerical investigation on the influence of EGR in a supercharged SI engine fueled with gasoline and alternative fuels. Energy Convers Manag 2014;83:260–9. https://doi.org/10.1016/j.enconman.2014.03.031.
[2] Raj R, Kumar Singh D, Vachan TJ. Performance simulation and optimization of SI engine fueled with peach biomass-based producer gas and propane blend. Therm Sci Eng Prog 2023;41:101816. https://doi.org/10.1016/j.tsep.2023.101816.
[3] Wu CK, Law CK. On the determination of laminar flame speeds from stretched flames. Symposium on Combustion 1985;20:1941–9. https://doi.org/10.1016/S0082-0784(85)80693-7.
[4] Scholte TG, Vaags PB. The burning velocity of hydrogen-air mixtures and mixtures of some hydrocarbons with air. Combustion and Flame 1959;3:495–501. https://doi.org/10.1016/0010-2180(59)90055-0.
[5] Lewis B, Von Elbe G. Determination of the speed of flames and the temperature distribution in a spherical bomb from time-pressure explosion records. The Journal of Chemical Physics 1934;2:283–90. https://doi.org/10.1063/1.1749464.
[6] de Goey LPH, van Maaren A, Ouax RM. Short Communication: Stabilization of Adiabatic Premixed Laminar Flames on a Flat Flame Burner. Combustion Science and Technology 1993;92:201–7. https://doi.org/10.1080/00102209308907668.
[7] Davis SG, Quinard J, Searby G. Markstein numbers in counterflow, methane-and propane-air flames: a computational study. Combustion and Flame 2002;130:123–36.
[8] Amirante R, Distaso E, Tamburrano P, Reitz RD. Laminar flame speed correlations for methane, ethane, propane and their mixtures, and natural gas and gasoline for spark-ignition engine simulations. International Journal of Engine Research 2017;18:951–70.
[9] Metghalchi M, Keck JC. Laminar burning velocity of propane-air mixtures at high temperature and pressure. Combustion and Flame 1980;38:143–54. https://doi.org/10.1016/0010-2180(80)90046-2.
[10] Hassan MI, Aung KT, Faeth GM. Properties of Laminar Premixed CO / H 2 / Air Flames Introduction. Proceedings of the Combustion Institute 1997:13.
[11] Takizawa K, Takahashi A, Tokuhashi K, Kondo S, Sekiya A. Burning velocity measurement of fluorinated compounds by the spherical-vessel method. Combustion and Flame 2005;141:298–307. https://doi.org/10.1016/j.combustflame.2005.01.009.
[12] Huzayyin AS, Moneib HA, Shehatta MS, Attia AMA. Laminar burning velocity and explosion index of LPG-air and propane-air mixtures. Fuel 2008;87:39–57. https://doi.org/10.1016/j.fuel.2007.04.001.
[13] Tang C, Zheng J, Huang Z, Wang J. Study on nitrogen diluted propane-air premixed flames at elevated pressures and temperatures. Energy Convers Manag 2010;51:288–95. https://doi.org/10.1016/j.enconman.2009.09.024.
[14] Brînzea V, Răzuş D, Mîţu M, Oancea D. Overall activation energy of propane-air combustion in laminar flames. Ars Docendi Publ House 2009;1:35–41.
[15] Brinzea V, Mitu M, Razus D, Oancea D. Overall activation parameters of propane oxidation in flames from normal burning velocities. Revue Roumaine de Chimie 2010;55:55–61.
[16] Brinzea V, Mitu M, Movileanu C, Musuc A, Razus D. Expansion coefficients and normal burning velocities of propane-air mixtures by the closed vessel technique. Buchar Univ Chem Fac Ann 2010;19:31–7.
[17] Brinzea V, Mitu M, Movileanu C, Razus D, Oancea D. Deflagration parameters of stoichiometric propane-air mixture during the initial stage of gaseous explosions in closed vessels. Revista de Chimie 2011;62:201–5.
[18] Razus D, Brinzea V, Mitu M, Movileanu C, Oancea D. Burning velocity of propane-air mixtures from pressure-time records during explosions in a closed spherical vessel. Energy & Fuels 2012;26:901–9. https://doi.org/10.1021/ef201561r.
[19] Yelishala SC, Wang Z, Metghalchi H, Levendis YA, Kannaiyan K, Sadr R. Effect of Carbon Dioxide on the Laminar Burning Speed of Propane-Air Mixtures. J Energy Resour Technol Trans ASME 2019:141. https://doi.org/10.1115/1.4042411.
[20] Wang Z, Lu Z, Yelishala SC, Metghalchi H, Levendis YA. Flame characteristics of propane-air-carbon dioxide blends at elevated temperatures and pressures. Energy 2021;228:120624. https://doi.org/10.1016/j.energy.2021.120624.
[21] Jomaas G, Zheng XL, Zhu DL, Law CK. Experimental determination of counterflow ignition temperatures and laminar flame speeds of C2–C3 hydrocarbons at atmospheric and elevated pressures. Proceedings of the Combustion Institute 2005;30:193–200. https://doi.org/10.1016/j.proci.2004.08.228.
[22] Akram M, Kishore VR, Kumar S. Laminar burning velocity of propane/CO 2/N 2-air mixtures at elevated temperatures. Energy & Fuels 2012;26:5509–18. https://doi.org/10.1021/ef301000k.
[23] Goswami M, Bastiaans RJM, De Goey LPH, Konnov AA. Experimental and modelling study of the effect of elevated pressure on ethane and propane flames. Fuel 2016;166:410–8. https://doi.org/10.1016/j.fuel.2015.11.013.
[24] Gu XJ, Haq MZ, Lawes M, Woolley R. Laminar burning velocity and Markstein lengths of methane-air mixtures. Combustion and Flame 2000;121:41–58. https://doi.org/10.1016/S0010-2180(99)00142-X.
[25] Wang Y, Movaghar A, Wang Z, Liu Z, Sun W, Egolfopoulos FN, et al. Laminar flame speeds of methane/air mixtures at engine conditions: Performance of different kinetic models and power-law correlations. Combustion and Flame 2020;218:101–8.
[26] Varghese RJ, Kolekar H, Kishore VR, Kumar S. Measurement of laminar burning velocities of methane-air mixtures simultaneously at elevated pressures and elevated temperatures. Fuel 2019:257. https://doi.org/10.1016/j.fuel.2019.116120.
[27] Wang H. Combustion Kinetics Laboratory Aerospace and Mechanical Engineering High-Temperature Combustion Reaction Model of H 2 /CO/C1-C4 Compounds Validation tests Ignition Delays Species Profiles in Shock-Tube Oxidation Laminar Flame Speeds Flow Reactor Burner St 2007:2007.
[28] Williams F. Chemical-kinetic mechanisms for combustion applications. San Diego Mechanism web page, Mechanical and Aerospace Engineering (Combustion Research), at San Diego.(2018) 2014.
[29] Qin Z, Lissianski VV, Yang H, Gardiner WC, Davis SG, Wang H. Combustion chemistry of propane: A case study of detailed reaction mechanism optimization. Proceedings of the Combustion Institute 2000;28:1663–9. https://doi.org/10.1016/S0082-0784(00)80565-2.
[30] Akram M, Minaev S, Kumar S. Investigations on the formation of planar flames in mesoscale divergent channels and prediction of burning velocity at high temperatures. Combustion Science and Technology 2013;185:645–60. https://doi.org/10.1080/00102202.2012.739224.
[31] Varghese RJ, Kolekar H, Hariharan V, Kumar S. Effect of CO content on laminar burning velocities of syngas-air premixed flames at elevated temperatures. Fuel 2018;214:144–53. https://doi.org/10.1016/j.fuel.2017.10.131.
[32] Maruta K, Kataoka T, Kim N, Minaev S, Fursenko R. Characteristics of combustion in a narrow channel with a temperature gradient. Proc Combust Inst 2005;30 II:2429–36. Doi: 10.1016/j.proci.2004.08.245.
[33] Kumar S, Maruta K, Minaev S, Fursenko R. Appearance of target pattern and spiral flames in radial microchannels with CH4-air mixtures. Physics of Fluids 2008;20.. https://doi.org/10.1063/1.2836670.
[34] Paidi SK, Bhavaraju A, Akram M, Kumar S. Effect of N2/CO2 dilution on laminar burning velocity of H2-air mixtures at high temperatures. International Journal of Hydrogen Energy 2013;38:13812–21. https://doi.org/10.1016/j.ijhydene.2013.08.024.

[35] Varghese RJ, Kolekar H, Kumar S. Demarcation of reaction effects on laminar burning velocities of diluted syngas–air mixtures at elevated temperatures. International Journal of Chemical Kinetics 2019;51:95–104. https://doi.org/10.1002/kin.21232.
[36] Varghese RJ, Kolekar H, Kumar S. Laminar burning velocities of H2/CO/CH4/CO2/N2 -air mixtures at elevated temperatures. International Journal of Hydrogen Energy 2019;44:12188–99. https://doi.org/10.1016/j.ijhydene.2019.03.103.
[37] Alekseev VA, Christensen M, Konnov AA. The effect of temperature on the adiabatic burning velocities of diluted hydrogen flames: A kinetic study using an updated mechanism. Combustion and Flame 2015;162:1884–98. https://doi.org/10.1016/j.combustflame.2014.12.009.
[38] Kee RJ, Rupley FM, Miller JA, Coltrin ME, Grcar JF, Meeks E, et al. CHEMKIN collection, release 3.6, reaction design. Inc, San Diego, CA 2000;20:0.
[39] Kuo KK. Principles of combustion 1986.
[40] Han P, David Checkel M, Fleck BA, Nowicki NL. Burning velocity of methane/diluent mixture with reformer gas addition. Fuel 2007;86:585–96. https://doi.org/10.1016/j.fuel.2006.08.011.
[41] Turányi T. Applications of sensitivity analysis to combustion chemistry. Reliability Engineering and System Safety 1997;57:41–8.
[42] Kong A. Reduced Kinetic Mechanism of Methane Oxidation for Rocket Applications 2015.
[43] Turányi T, Tomlin AS. Analysis of kinetic reaction mechanisms, vol. 20. Springer; 2014.
[44] Ellson J, Gansner E, Koutsofios L, North SC, Woodhull G, Graphviz—open source graph drawing tools. Graph Draw. 9th Int. Symp. GD,. Vienna, Austria, Sept. 23–26, 2001 Revis. Pap. 9. Springer 2001;2002:483–4.
[45] Goodwin DG, Moffat HK, Speth RL. Cantera: An object-oriented software toolkit for chemical kinetics, thermodynamics, and transport processes 2018.
[46] Van Rossum G. Python Programming Language. USENIX Annu. Tech. Conf., vol. 41, Santa Clara, CA; 2007, p. 1–36.